The endosomal adaptor protein APPL1 impairs the turnover of leading edge adhesions to regulate cell migration

Joshua A. Broussard[a], Wan-hsin Lin[a], Devi Majumdar[a], Bridget Anderson[a], Brady Eason[b], Claire M. Brown[b], and Donna J. Webb[a,c]

[a]Department of Biological Sciences and Vanderbilt Kennedy Center for Research on Human Development, Nashville, TN 37235; [b]Life Sciences Complex Imaging Facility, McGill University, Montreal, QC H3G 0B1, Canada; [c]Department of Cancer Biology, Vanderbilt University, Nashville, TN 37235

ABSTRACT **Cell migration is a complex process that requires the integration of signaling events that occur in distinct locations within the cell. Adaptor proteins, which can localize to different subcellular compartments, where they bring together key signaling proteins, are emerging as attractive candidates for controlling spatially coordinated processes. However, their function in regulating cell migration is not well understood. In this study, we demonstrate a novel role for the adaptor protein containing a pleckstrin-homology (PH) domain, phosphotyrosine-binding (PTB) domain, and leucine zipper motif 1 (APPL1) in regulating cell migration. APPL1 impairs migration by hindering the turnover of adhesions at the leading edge of cells. The mechanism by which APPL1 regulates migration and adhesion dynamics is by inhibiting the activity of the serine/threonine kinase Akt at the cell edge and within adhesions. In addition, APPL1 significantly decreases the tyrosine phosphorylation of Akt by the nonreceptor tyrosine kinase Src, which is critical for Akt-mediated cell migration. Thus, our results demonstrate an important new function for APPL1 in regulating cell migration and adhesion turnover through a mechanism that depends on Src and Akt. Moreover, our data further underscore the importance of adaptor proteins in modulating the flow of information through signaling pathways.**

Monitoring Editor
Josephine C. Adams
University of Bristol

Received: Feb 10, 2011
Revised: Feb 15, 2012
Accepted: Feb 23, 2012

INTRODUCTION

Adaptor proteins are emerging as important regulators of key signaling events that control cellular behaviors underlying many biological and pathological processes (Flynn, 2001). They can accomplish this through their multiple functional domains by bringing together and targeting protein-binding partners to specific locations within cells (Pawson, 2007). This capability places adaptor proteins in an ideal position to integrate and direct signals that control highly complex, spatiotemporally regulated processes such as cell migration. Indeed, recent work has pointed to a role for these integrators in the regulation of cell migration (Nayal *et al.*, 2006; Yu *et al.*, 2009; Meenderink *et al.*, 2010; Deakin and Turner, 2011); however, their function in modulating this process is not well understood.

The adaptor protein containing a pleckstrin-homology (PH) domain, phosphotyrosine-binding (PTB) domain, and leucine zipper motif 1 (APPL1) is a 709–amino acid endosomal protein that was first identified through its association with Akt (also known as protein kinase B) in a yeast two-hybrid screen (Mitsuuchi *et al.*, 1999). APPL1 contains an N-terminal Bin-Amphiphysin-Rvs (BAR) domain, a central PH domain, and a C-terminal PTB domain (Mitsuuchi *et al.*, 1999; Miaczynska *et al.*, 2004). The BAR domain is a dimerization motif associated with sensing and/or induction of membrane curvature (Habermann, 2004; Peter *et al.*, 2004; Chial *et al.*, 2010). Similarly, the PH and PTB domains of APPL1 have been reported to

This article was published online ahead of print in MBoC in Press (http://www.molbiolcell.org/cgi/doi/10.1091/mbc.E11-02-0124) on February 29, 2012.

Address correspondence to: Donna J. Webb (donna.webb@vanderbilt.edu).

Abbreviations used: APPL1, adaptor protein containing a pleckstrin-homology domain, phosphotyrosine-binding domain, and leucine zipper motif 1; BAR, Bin-Amphiphysin-Rvs; CA, constitutively active; DCC, deleted in colorectal cancer; DMEM, Dulbecco's modified Eagle's medium; DN, dominant-negative; FBS, fetal bovine serum; FRET, fluorescence resonance energy transfer; HGF, hepatocyte growth factor; IB, immunoblot; IP, immunoprecipitate; MEF, murine embryonic fibroblast; PBS, phosphate-buffered saline; PH, pleckstrin-homology; PTB, phosphotyrosine-binding; SEM, standard error of the mean; siRNA, small interfering RNA; TIRF, total internal reflection microscopy.

bind to phosphoinositol lipids (Li *et al.*, 2007; Chial *et al.*, 2008). The BAR and PH domains of APPL1 cooperate to form a functionally unique BAR-PH domain that differentiates it from other members of the BAR domain–containing protein family (Li *et al.*, 2007; Zhu *et al.*, 2007). APPL1 interacts with the early endosomal protein Rab5 via the BAR-PH domain (Miaczynska *et al.*, 2004; Zhu *et al.*, 2007). Moreover, the PTB domain is the critical region of APPL1 that is responsible for binding Akt (Mitsuuchi *et al.*, 1999).

Akt is a serine/threonine kinase that is activated downstream of phosphatidylinositol 3-kinase (PI3K; Franke *et al.*, 1995). PI3K signaling recruits Akt to the plasma membrane, where it becomes activated following phosphorylation on two conserved residues, threonine 308 (T308) and serine 473 (S473) (Alessi *et al.*, 1996). Of interest, Akt activation also occurs on signaling endosomes, whereby PI3K is recruited to endosomal membranes and promotes the activation of Akt (Wang *et al.*, 2002). Active Akt phosphorylates its downstream effectors to regulate several cellular processes, including cell growth, survival, and proliferation (Manning and Cantley, 2007). Moreover, there has recently been growing interest in the function of Akt in the regulation of cell migration. Akt has been shown to stimulate the migration of epithelial cells, fibroblasts, and fibrosarcomas and to promote the invasion of breast carcinomas and fibrosarcomas (Kim *et al.*, 2001; Irie *et al.*, 2005; Zhou *et al.*, 2006; Ju *et al.*, 2007).

In addition to the regulatory phosphorylation at T308 and S473, recent work has shown that Akt also undergoes tyrosine phosphorylation (Chen *et al.*, 2001). Akt tyrosine phosphorylation is mediated by the non-receptor tyrosine kinase Src (Chen *et al.*, 2001). Src-mediated tyrosine phosphorylation of Akt is reported to be important in both the activation and function of Akt (Chen *et al.*, 2001; Choudhury *et al.*, 2006; Bouchard *et al.*, 2007). However, nothing is known about the role of Akt tyrosine phosphorylation in the regulation of cell migration.

Cell migration is initiated in response to an external stimulus and begins with the extension of an actin-rich protrusion, which is stabilized by the formation of nascent adhesions at the leading edge (Carson *et al.*, 1986; Zaidel-Bar *et al.*, 2003; Ponti *et al.*, 2004; Nayal *et al.*, 2006). These adhesions can then mature into large, stable adhesions through subsequent recruitment of signaling, adaptor, and cytoskeleton-related proteins, or they can disassemble (Miyamoto *et al.*, 1995; Zaidel-Bar *et al.*, 2007; Choi *et al.*, 2008; Dubash *et al.*, 2009; Kanchanawong *et al.*, 2010). For migration to proceed in an efficient manner, adhesions at the leading edge of the cell must continually form (assemble) and disassemble in a process termed adhesion turnover (Laukaitis *et al.*, 2001; Webb *et al.*, 2004; Dubash *et al.*, 2009).

Here we show that the adaptor protein APPL1 is an important regulator of cell migration and adhesion dynamics. APPL1 modulates these processes in a manner that depends on its ability to regulate Akt activity and function. Moreover, APPL1 inhibits the ability of Akt to promote migration by impairing Src-mediated tyrosine phosphorylation of Akt.

RESULTS

The signaling adaptor APPL1 inhibits cell migration

The multidomain adaptor protein APPL1 (Figure 1A) has been shown to interact with various signaling and trafficking proteins, putting it in an ideal position to spatiotemporally coordinate signaling pathways that underlie processes such as cell migration. This led us to hypothesize that APPL1 is an important regulator of migration. To begin to test our hypothesis, we expressed green fluorescent protein (GFP) and GFP-APPL1 in HT1080 cells, plated them on fibronectin, and assessed their migration using live-cell imaging. The migration of individual cells was tracked using MetaMorph software, and Rose plots were generated from these data (Figure 1B). The migration paths for GFP-APPL1–expressing cells were significantly shorter than those of control cells expressing GFP, suggesting that APPL1 decreased the rate of migration in HT1080 cells (Figure 1B). Indeed, quantification of the migration speed revealed a 1.7-fold decrease in GFP-APPL1–expressing cells compared with control cells expressing GFP (Figure 1B). To further show a function for APPL1 in migration, we expressed GFP-APPL1 in MDA-MB-231 cells, which have similar endogenous levels of APPL1 as HT1080 cells (Supplemental Figure S1A). As with HT1080 cells, expression of GFP-APPL1 significantly reduced the migration speed of MDA-MB-231 cells (Supplemental Figure S1B). Collectively, these results point to a role for APPL1 in the regulation of cell migration.

We continued to probe the function of APPL1 in modulating migration by generating two small interfering RNA (siRNA) constructs to knock down endogenous expression of this protein. Although APPL1 siRNA 1 had been reported to be very effective (Miaczynska *et al.*, 2004), we confirmed its ability to knock down expression of APPL1. When wild-type HT1080 cells were transfected with APPL1 siRNA 1, endogenous expression of APPL1 was decreased by >80% compared with either empty pSUPER vector or a scrambled siRNA, as determined by Western blot analysis (Figure 1C). APPL1 siRNA 2 similarly decreased endogenous levels of APPL1 by ~65% compared with empty pSUPER vector or a scrambled siRNA (Figure 1C), indicating the APPL1 siRNAs were effective in knocking down expression of APPL1. Transfection of HT1080 cells with APPL1 siRNA 1 and APPL1 siRNA 2 led to 1.4- and 1.3-fold increase in migration speed, respectively, compared with pSUPER or scrambled siRNA transfected cells (Figure 1D). These results indicate that decreased expression of APPL1 enhances cell migration, thus implicating APPL1 as an important regulator of this process.

Endosomal localization of APPL1 is required for its effects on migration

Because APPL1 localizes to early endosomes and signaling events that take place on endosomes are increasingly believed to play important roles in modeling cellular behavior (Miaczynska *et al.*, 2004; von Zastrow and Sorkin, 2007), we hypothesized the APPL1 localization to endosomes is critical for its ability to regulate cell migration. To determine whether APPL1 endosomal localization was necessary for its effects on migration, we mutated three basic residues (R147A, K153A, and K155A) within the BAR domain of APPL1 that had previously been shown to be sufficient to disrupt its endosomal localization (Schenck *et al.*, 2008). GFP-APPL1, like endogenous APPL1, localized to vesicular structures; however, GFP-APPL1 that contained the point mutations (GFP-APPL1-AAA) no longer localized to endosomes when expressed in HT1080 cells (Figure 2, A and B). The migration speed of cells expressing GFP-APPL1-AAA was not significantly different from that of control GFP-expressing cells (Figure 2, C and D). These results suggest that the localization of APPL1 to endosomal membranes is critical for its ability to regulate cell migration.

APPL1 regulates leading edge adhesion dynamics in migrating cells

Adhesion assembly and disassembly at the leading edge of cells—termed adhesion turnover—is required for efficient migration to occur (Webb *et al.*, 2004; Nayal *et al.*, 2006). This led us to hypothesize that APPL1 affects migration through its ability to regulate adhesion turnover. To determine whether APPL1 affects the number and/or size of adhesions, we expressed GFP and GFP-APPL1 in wild-type HT1080 cells and immunostained for endogenous paxillin, which is

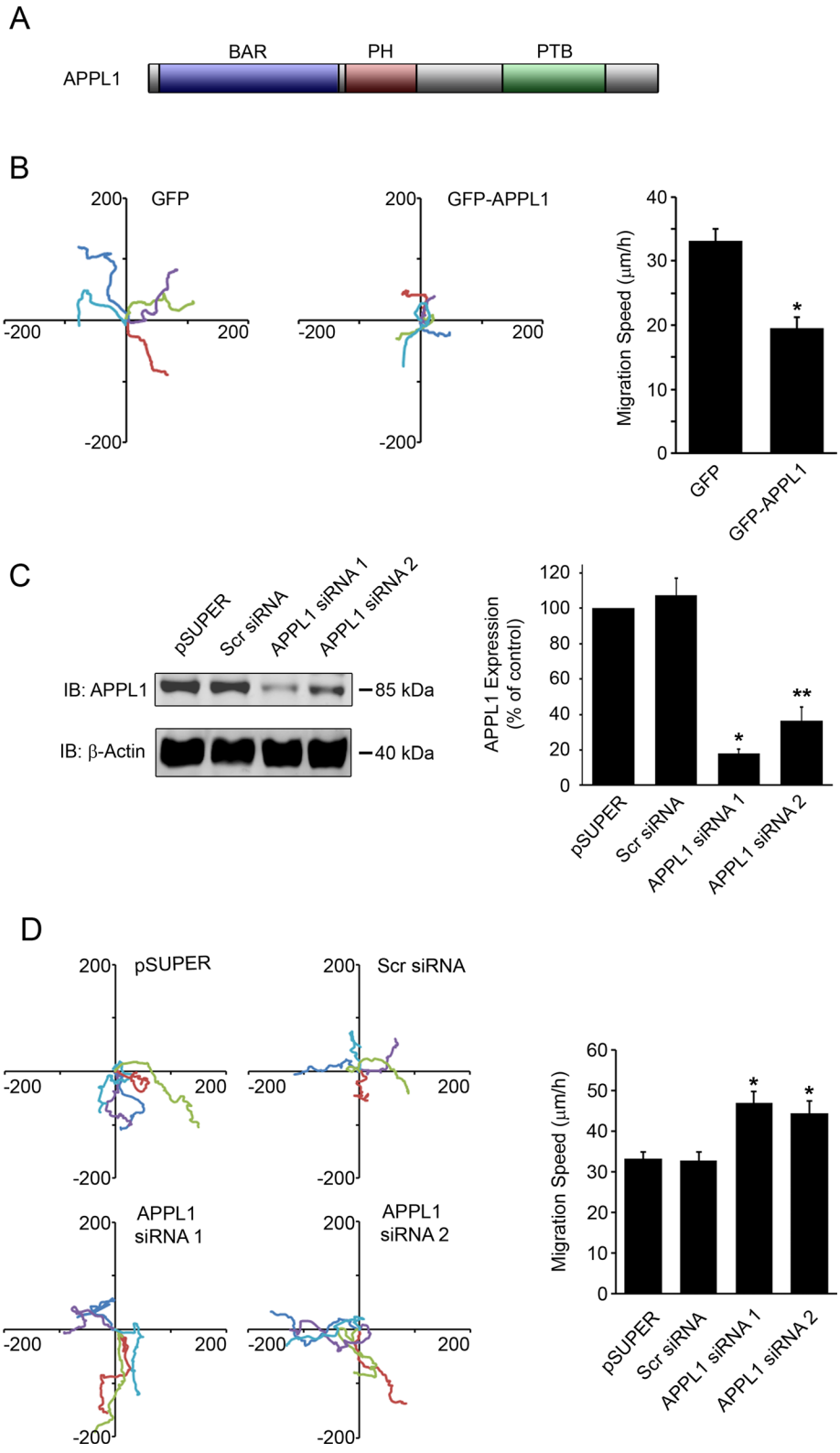

FIGURE 1: APPL1 regulates cell migration. (A) A schematic with the domain structure of APPL1. (B) HT1080 cells were transfected with either GFP or GFP-APPL1, plated on fibronectin, and subjected to time-lapse microscopy. Migration was quantified for individual cells, and Rose plots of migration tracks are shown (left). Quantification of the migration speed for GFP- and GFP-APPL1–expressing cells is shown (right). Error bars represent the standard error of the mean (SEM) for 49–64 cells from at least three separate experiments (*$p < 0.0001$). (C) HT1080 cells were transfected with empty pSUPER vector, a scrambled siRNA (Src siRNA), or APPL1 siRNA. Cell lysates were subjected to immunoblot analysis to determine the levels of endogenous APPL1 and β-actin (as a loading control; left). Quantification of the endogenous levels of APPL1 in cells transfected with the indicated constructs is shown (right). Error bars represent the SEM from four separate experiments (*$p < 0.0001$, **$p = 0.0002$). (D) Cells were transfected with empty pSUPER vector, a scrambled siRNA (Src siRNA), or APPL1 siRNA and used in migration assays 3 d later. Left, Rose plots with migration tracks for cells transfected with the indicated constructs. Right, quantification of the migration speed of cells transfected with the indicated constructs. Error bars represent the SEM for 46–64 cells from three individual experiments (*$p < 0.0009$). For C and D, asterisks indicate a statistically significant difference compared with pSUPER-transfected cells.

a well-characterized adhesion marker. Cells expressing GFP-APPL1 exhibited a greater number of larger central adhesions and fewer nascent peripheral adhesions compared with control cells expressing GFP (Figure 3A). In GFP-APPL1–expressing cells, the larger central adhesions could arise from their inability to efficiently turn over. We examined this possibility by quantitatively measuring adhesion turnover using an assay that we previously developed (Webb *et al.*, 2004). GFP- and GFP-APPL1–expressing cells that were transfected with mCherry-paxillin were subjected to time-lapse fluorescence microscopy, and the $t_{1/2}$ values for adhesion assembly and disassembly were assessed (Webb *et al.*, 2004). Cells expressing GFP-APPL1 exhibited a 1.8-fold increase in the apparent $t_{1/2}$ for adhesion assembly as compared with GFP controls (Figure 3, B and C), indicating that adhesions are forming considerably more slowly in the GFP-APPL1–expressing cells. Moreover, GFP-APPL1 expression led to a 1.4-fold increase in the $t_{1/2}$ for adhesion disassembly (Figure 3, B and C).

In addition, we used the adhesion turnover assay to examine the effects of GFP-APPL1-AAA on adhesion dynamics. Cells expressing this mislocalization mutant had assembly and disassembly $t_{1/2}$ values of 2.1 ± 0.3 and 3.0 ± 0.3 min, respectively, which are not significantly different from those observed in GFP controls (Figure 3C). Taken together, these results demonstrate that APPL1 significantly slows the rate of adhesion assembly and disassembly in cells in a manner dependent on its endosomal localization.

We further corroborated a role for APPL1 in modulating adhesion turnover by knocking down expression of the endogenous protein. Expression of APPL1 siRNA 1 and APPL1 siRNA 2 decreased the apparent $t_{1/2}$ of adhesion assembly by 1.4- and 1.5-fold, respectively, compared with both scrambled siRNA and GFP controls

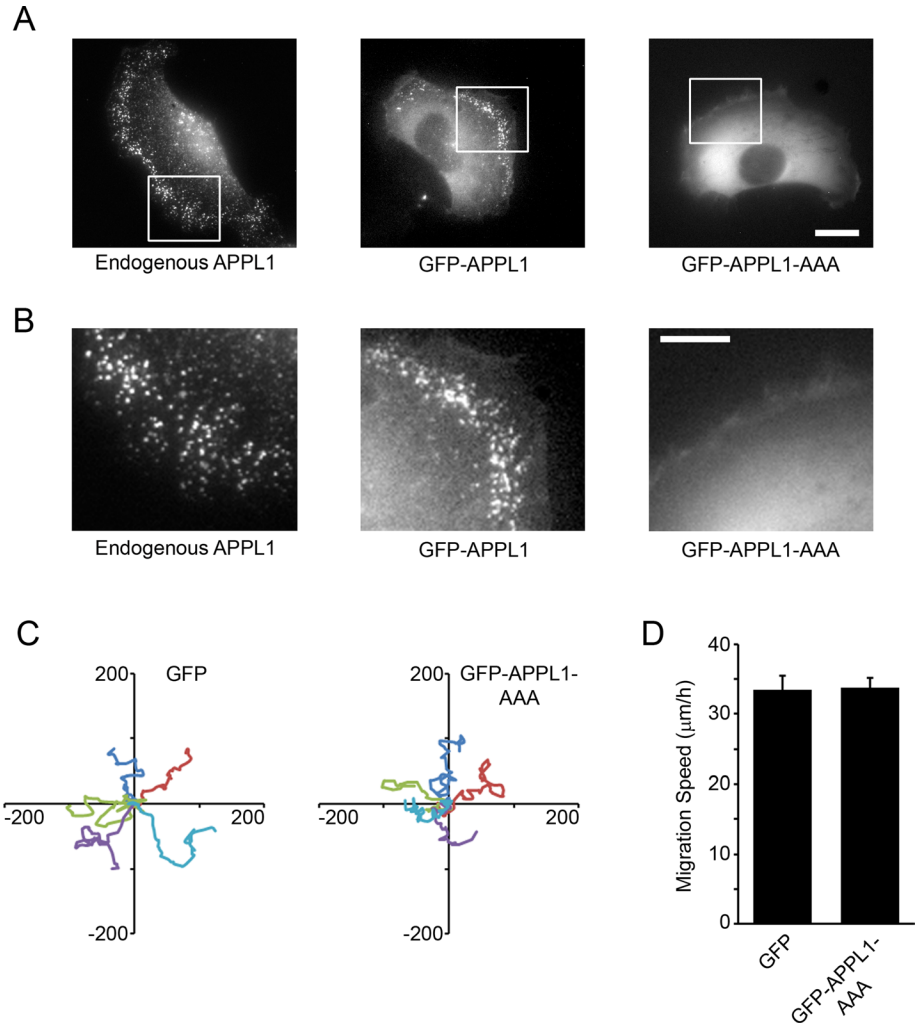

FIGURE 2: APPL1 localizes to vesicular structures, which is critical in its regulation of cell migration. (A) Wild-type HT1080 cells were immunostained for endogenous APPL1 (left) or transfected with either GFP-APPL1 (middle) or GFP-APPL1 in which three basic residues (147, 153, and 155) within the BAR domain were mutated to alanines (GFP-APPL1-AAA; right). Unlike GFP-APPL1 or the endogenous protein, GFP-APPL1-AAA did not localize to endosomal structures. Scale bar, 15 μm. (B) High-magnification images of the boxed regions from A. Scale bar, 15 μm. (C) GFP- and GFP-APPL1-AAA–transfected cells were imaged using time-lapse microscopy, and migration was analyzed. Rose plots with migration tracks for these cells are shown. (D) Quantification of the migration speed of GFP- and GFP-APPL1-AAA–expressing cells. Error bars represent the SEM for 52–66 cells from at least three separate experiments.

(Figure 3C). In addition, APPL1 siRNA 1 and APPL1 siRNA 2 decreased the $t_{1/2}$ of adhesion disassembly by 1.7- and 1.8-fold, respectively, as compared with controls (Figure 3C). These results reveal that cells turn over their adhesions much faster when endogenous APPL1 expression is decreased, indicating an inhibitory role for APPL1 in the regulation of leading edge adhesion dynamics.

APPL1 and Akt regulate cell migration and adhesion dynamics

Because Akt was previously shown to interact with APPL1 and Akt has been implicated as a regulator of cell migration (Mitsuuchi *et al.*, 1999; Kim *et al.*, 2001; Arboleda *et al.*, 2003; Irie *et al.*, 2005; Zhou *et al.*, 2006; Ju *et al.*, 2007; Schenck *et al.*, 2008), APPL1 may affect migration via a mechanism involving Akt. Since the PTB domain of APPL1 mediates its interaction with Akt (Mitsuuchi *et al.*, 1999; Schenck *et al.*, 2008), we expressed a GFP-APPL1 truncation mutant that lacked the PTB domain (GFP-APPL1-ΔPTB) and assessed migration using time-lapse microscopy. Expression of GFP-APPL1 significantly decreased the rate of migration compared with control GFP-expressing cells (Supplemental Figure S2, A and B). However, the APPL1-induced decrease in migration was abolished in GFP-APPL1-ΔPTB–expressing cells, whose migration speed was similar to that observed in GFP control cells (Supplemental Figure S2, A and B). This suggests that Akt contributes to the effect of APPL1 on cell migration.

We further investigated the relationship between APPL1 and Akt in the regulation of cell migration by using a mutant-based approach. We expressed either a dominant-negative (DN-Akt) or a constitutively active Akt1 mutant (CA-Akt) in wild-type HT1080 cells and analyzed migration using time-lapse microscopy. Cells expressing DN-Akt showed a 1.7-fold decrease in their speed of migration as compared with control cells (Figure 4, A and B). In contrast, cells expressing CA-Akt exhibited a 1.3-fold increase in migration as compared with controls (Figure 4, A and B). Of interest, the migration speed of cells coexpressing either GFP-APPL1 and DN-Akt or GFP-APPL1 and CA-Akt did not significantly differ from that of cells expressing GFP-APPL1 alone (Figure 4, A and B). These results indicate that GFP-APPL1 expression can suppress the CA-Akt–induced increase in migration, whereas it does not provide an additive effect on migration when coexpressed with DN-Akt.

To further investigate the ability of APPL1 to suppress Akt-induced migration, we generated stable HT1080 cells expressing either GFP or GFP-APPL1. In the stable GFP-APPL1 cells, the level of APPL1 expression was 1.5-fold over the endogenous protein (Figure 4C). This expression level was comparable to that obtained with our transient transfections in which GFP-APPL1 was expressed at 1.9-fold over endogenous (Figure 4C). The GFP-APPL1 stable cells were then transfected with CA-Akt. As with the transient transfections, expression of CA-Akt (3.1-fold over endogenous Akt; Figure 4D) did not significantly affect the migration of GFP-APPL1 stable cells (Figure 4E). However, when the expression level of CA-Akt was increased to 5.3-fold over endogenous Akt (2X CA-Akt; Figure 4D), the migration speed of the GFP-APPL1 stable cells was increased (Figure 4E). These results indicate that although GFP-APPL1 expression can inhibit low levels of CA-Akt from promoting migration, higher expression of CA-Akt can overcome this inhibition.

We next generated two siRNA constructs to knock down endogenous Akt. Although we previously used these two siRNA sequences to effectively knock down endogenous Akt (Bristow *et al.*, 2009), we confirmed their efficacy by transfecting them into HT1080 cells. Here, we obtained similar results, in which Akt siRNA 1 knocked down endogenous Akt to 61.8 ± 9.4% of control levels, whereas Akt siRNA 2 had an efficacy of 51.9 ± 4.7% (n = 4 separate experiments for each siRNA).

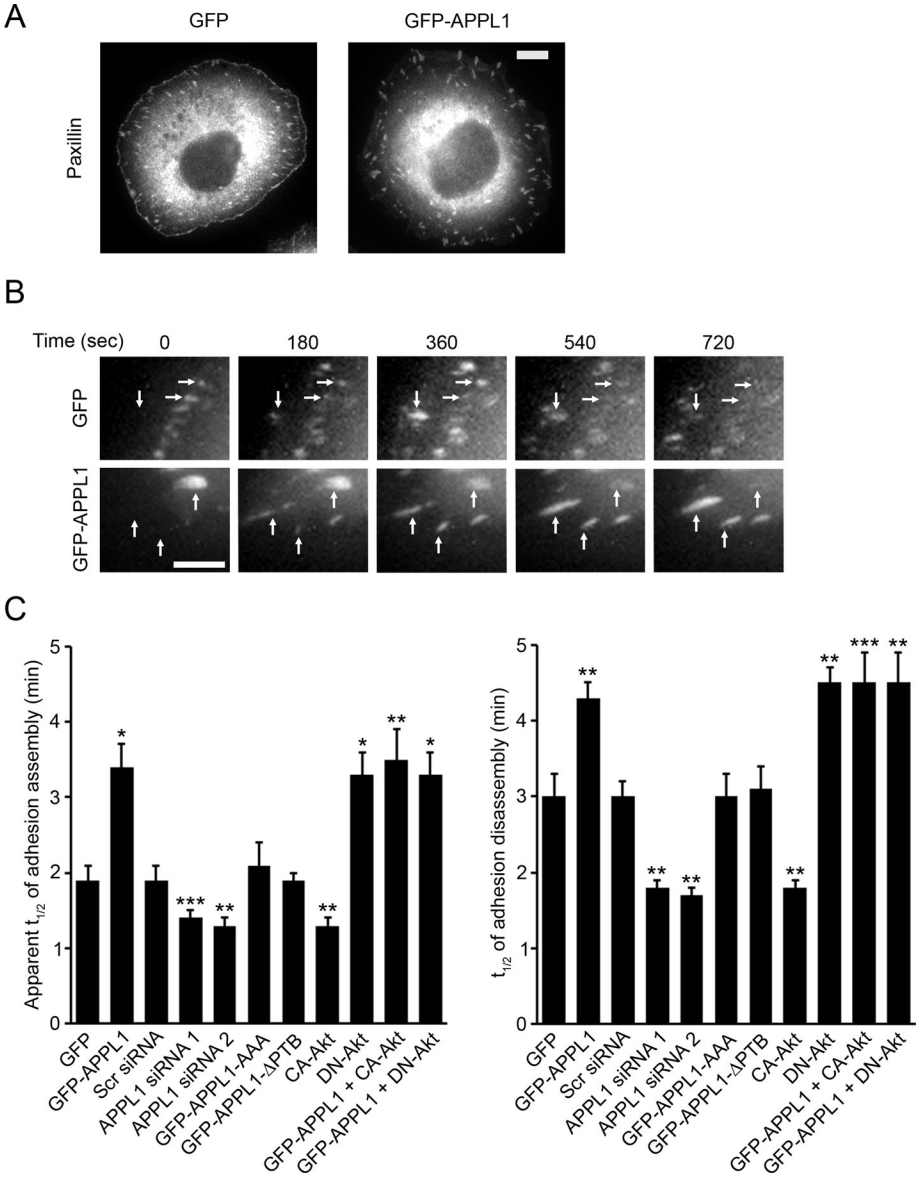

FIGURE 3: APPL1 impairs adhesion turnover at the leading edge of cells. (A) Cells were transfected with either GFP or GFP-APPL1 and immunostained for the adhesion marker paxillin. Scale bar, 10 μm. (B) HT1080 cells were cotransfected with mCherry-paxillin and either GFP or GFP-APPL1 and imaged using time-lapse microscopy. In GFP-APPL1–expressing cells, the leading edge adhesions assemble and disassemble more slowly than those in control cells expressing GFP (arrows). Scale bar, 5 μm. (C) Quantification of the apparent $t_{1/2}$ for adhesion assembly and the $t_{1/2}$ for adhesion disassembly for cells expressing the indicated constructs. Error bars represent the SEM for 26–30 adhesions from four to six cells from at least three independent experiments (*$p < 0.0001$, **$p \leq 0.007$, ***$p < 0.013$). Asterisks indicate a statistically significant difference compared with GFP cells.

Migration was then analyzed to determine the effect of these constructs on this process. Cells transfected with Akt siRNA 1 exhibited a 1.5-fold decrease in migration speed compared with either empty pSUPER vector or scrambled siRNA-expressing cells (Figure 5, A and B). Similarly, Akt siRNA 2-transfected cells showed a 1.6-fold decrease in migration speed compared with controls (Figure 5, A and B). Moreover, expression of GFP-APPL1 along with Akt knockdown showed no further effect on migration (Figure 5, A and B), which is consistent with the results obtained when GFP-APPL1 was coexpressed with DN-Akt (Figure 4, A and B). Taken together, these results suggest that APPL1 is regulating cell migration by inhibiting Akt function.

Because our results indicated that the APPL1-Akt association is critical in the regulation of cell migration, we assessed the effect of APPL1 and Akt on adhesion turnover. In cells expressing GFP-APPL1-ΔPTB, the apparent $t_{1/2}$ for adhesion assembly and the $t_{1/2}$ for adhesion disassembly were similar to those obtained for GFP control cells, indicating that deletion of the PTB domain of APPL1 abolished its effect on adhesion turnover (Figure 3C). We further probed the role of APPL1 and Akt in modulating adhesion dynamics by coexpressing Akt mutants with GFP or GFP-APPL1. Expression of CA-Akt decreased the $t_{1/2}$ of adhesion assembly and disassembly as compared with GFP control cells, whereas DN-Akt expression led to a significant increase in the $t_{1/2}$ values (Figure 3C). When GFP-APPL1 was coexpressed with the Akt mutants, the $t_{1/2}$ values were not significantly different from those observed in cells expressing GFP-APPL1 alone (Figure 3C). Thus, as with migration, APPL1 inhibits the function of CA-Akt in regulating adhesion turnover, while providing no additional effect on adhesion dynamics when coexpressed with DN-Akt.

APPL1 reduces the amount of active Akt in cells

To begin to elucidate the mechanism by which the APPL1-Akt association regulates migration and adhesion dynamics, we examined the effect of APPL1 on the level of active Akt. Canonically, Akt is activated through phosphorylation on two amino acids, Thr-308 and Ser-473 (Alessi *et al.*, 1996), and thus phosphorylation-specific antibodies against these residues can be used to detect active Akt. Cells expressing GFP and GFP-APPL1 were immunostained with phospho–Thr-308-Akt antibody and imaged using fluorescence microscopy. The fluorescence intensity of active Akt was then quantified for individual cells using MetaMorph software. Expression of GFP-APPL1 reduced the level of active Akt by approximately twofold as compared with control cells expressing GFP (Supplemental Figure S3A). Knockdown of endogenous APPL1, using APPL1 siRNA 1 and APPL1 siRNA 2, increased the amount of active Akt by almost 1.5-fold compared with empty pSUPER vector, whereas scrambled siRNA had no significant effect on the level of active Akt (Supplemental Figure S3B). Of interest, the GFP-APPL1-ΔPTB mutant did not significantly affect the amount of active Akt in HT1080 cells (101.7 ± 3.3% of control, n = 85 cells), suggesting that an association between APPL1 and Akt is necessary for the APPL1 effect on active Akt. Moreover, the level of active Akt in GFP-APPL1-AAA–expressing cells was similar to that observed in GFP control cells (95.2 ± 3.4% of control, n = 145 cells), indicating that APPL1 regulates the amount of active Akt in cells in a manner dependent on its endosomal localization.

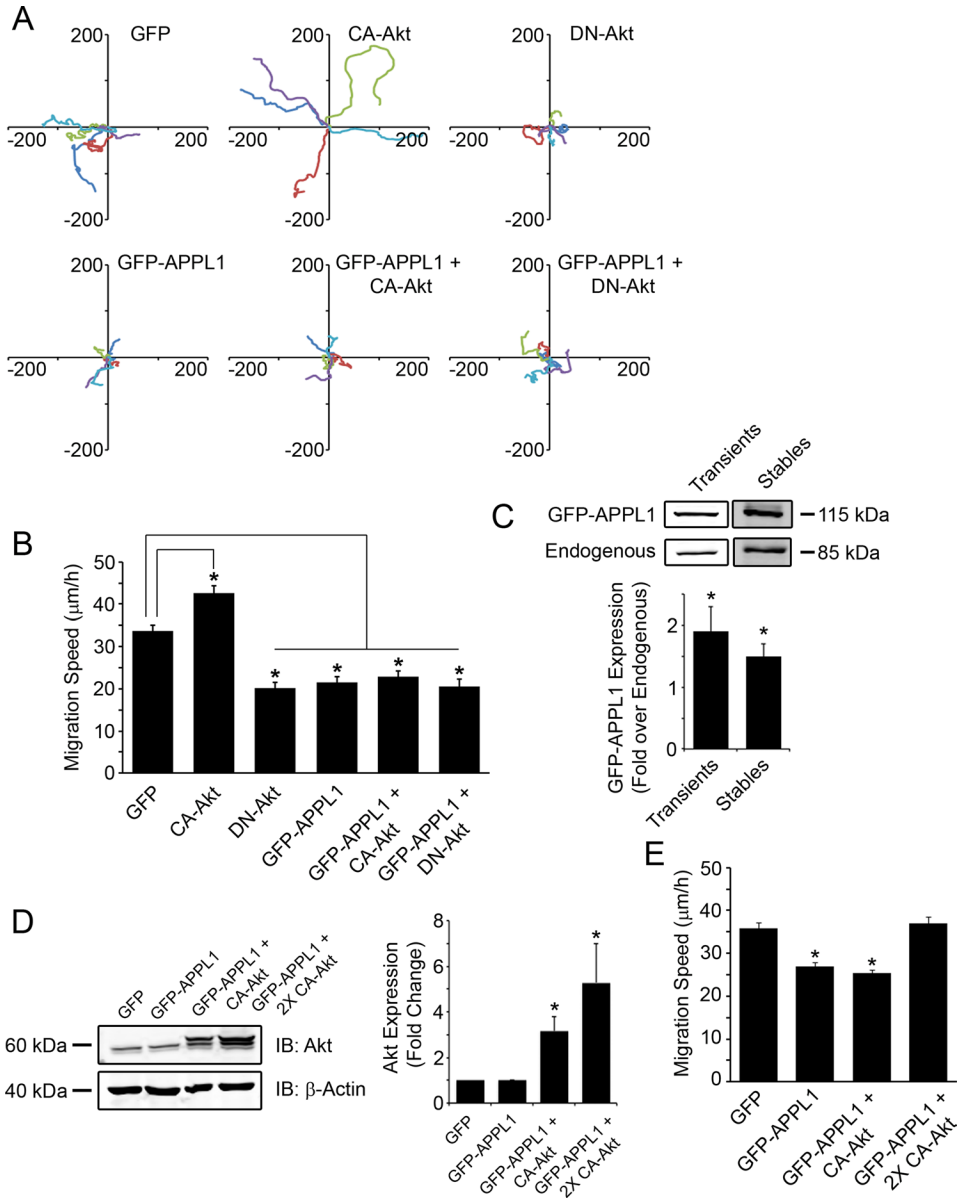

FIGURE 4: Akt plays an important role in the APPL1-mediated regulation of cell migration. (A) HT1080 cells were cotransfected with GFP or GFP-APPL1 and empty vector, constitutively active Akt (CA-Akt), or dominant-negative Akt (DN-Akt) and used in migration assays. Rose plots with individual migration tracks for cells transfected with the indicated constructs are shown. (B) Quantification of the migration speed of cells transfected with the indicated constructs. Error bars represent the SEM of 35–65 cells from at least three individual experiments (*$p < 0.0001$). (C) Lysates from HT1080 cells transiently transfected with GFP-APPL1 (Transients) and HT1080 cells stably expressing GFP-APPL1 (Stables) were subjected to immunoblot analysis to determine the levels of total APPL1 (endogenous and exogenously expressed GFP-APPL1; top). Quantification of the relative amounts of GFP-APPL1 compared with endogenous APPL1 is shown (bottom). Error bars represent the SEM from at least three separate experiments (*$p < 0.05$). Asterisks indicate a statistically significant difference compared with endogenous APPL1. (D) Stable HT1080 cells expressing GFP were transfected with empty vector (GFP). Stable HT1080 cells expressing GFP-APPL1 were transfected with empty vector (GFP-APPL1), 1.5 μg of CA-Akt cDNA (GFP-APPL1 + CA-Akt), or 3 μg of CA-Akt cDNA (GFP-APPL1 + 2X CA-Akt). Left, cell lysates were subjected to immunoblot analysis to determine the levels of total Akt (endogenous and exogenously expressed CA-Akt) and β-actin (as a loading control). Right, quantification of the relative amount of Akt expression compared with that observed in control GFP cells. Error bars represent the SEM from three separate experiments (*$p \leq 0.03$). Asterisks indicate a statistically significant difference compared with control GFP cells. (E) Stable HT1080 GFP or GFP-APPL1 cells were transfected as described in D and used in migration assays. Quantification of the migration speed of transfected cells is shown. Error bars represent the SEM of 80–91 cells from three individual experiments (*$p < 0.0001$). Asterisks indicate a statistically significant difference compared with GFP cells.

Collectively, these results indicate that APPL1 regulates the amount of active Akt in cells and point to an important role for this function of APPL1 in modulating cell migration.

We used a previously described Akind fluorescence resonance energy transfer (FRET) probe (Yoshizaki *et al.*, 2007) to further investigate the role of APPL1 in regulating Akt activity. Akind is

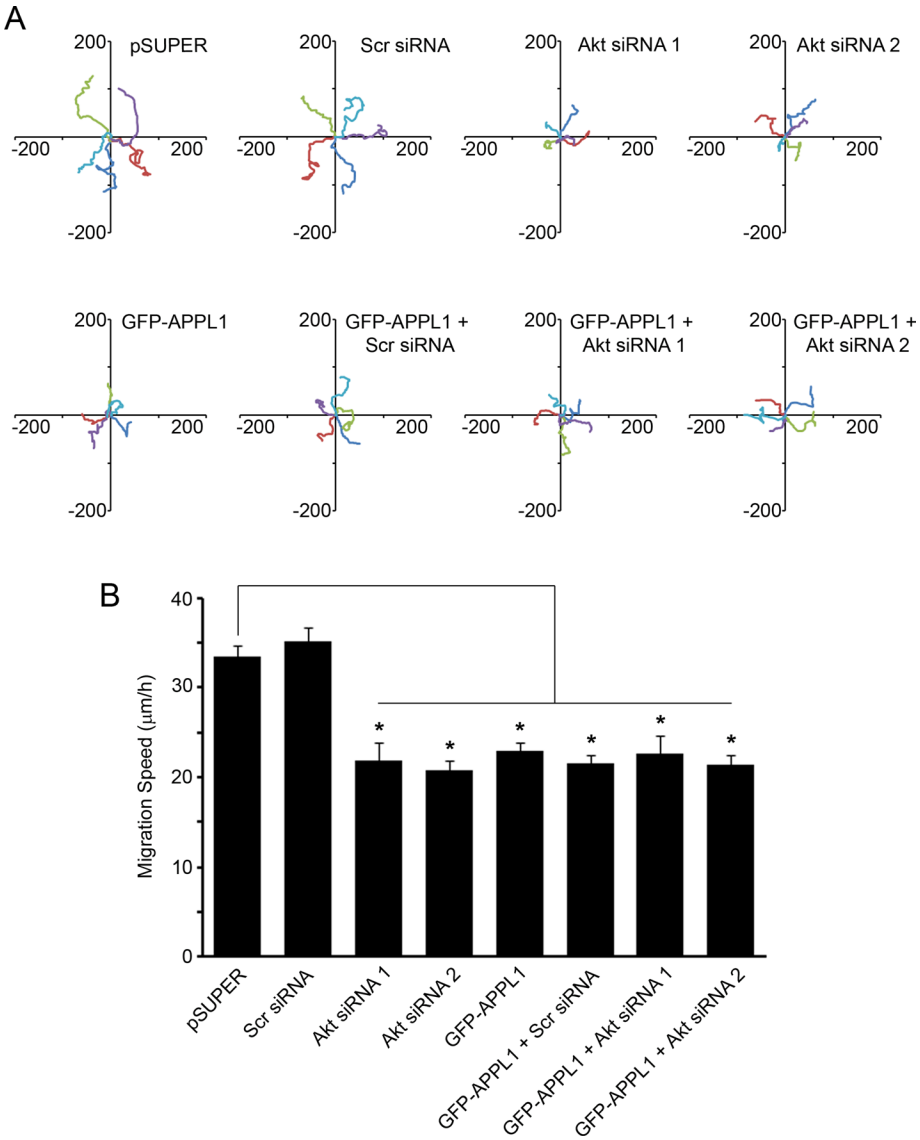

FIGURE 5: Akt knockdown inhibits cell migration. (A) HT1080 cells were cotransfected with empty pSUPER vector, a scrambled siRNA (Scr siRNA), or Akt siRNA and either GFP or GFP-APPL1 and imaged using time-lapse microscopy 3 d later. Rose plots are shown for the migration tracks of cells expressing the indicated constructs. (B) Quantification of the migration speed of cells transfected with the indicated constructs is shown. Error bars represent the SEM of 56–76 cells from three separate experiments (*$p < 0.0001$).

composed of the Akt PH domain (amino acids 1–144), the fluorescent protein Venus, the Akt catalytic and regulatory domains (amino acids 133–480), and cyan fluorescent protein (CFP; Yoshizaki *et al.*, 2007). On activation, Akind undergoes a conformational change that brings Venus and CFP into close enough proximity to undergo FRET. Cells expressing mCherry-APPL1 exhibited a 1.8-fold decrease in the average Akind FRET/CFP ratio when compared with mCherry-expressing control cells (Figure 6A). When we quantified Akt activity as a function of distance from the edge of cells, the FRET/CFP ratio in control cells was high at the cell edge (Figure 6B), indicating that active Akt was localized to this region. In mCherry-APPL1–expressing cells, the FRET/CFP ratio was decreased 2.9-fold at the cell edge compared with controls (Figure 6B). Akt activity was also decreased 2.2-fold at a distance of 5 μm behind the cell edge in mCherry-APPL1–expressing cells (Figure 6B). Taken together, these results indicate that APPL1 decreases the amount of active Akt in cells, and a significant reduction of Akt activity is seen at the cell edge.

Because APPL1 affected the level of active Akt at the cell edge, and APPL1 and Akt modulated the turnover of adhesions at the leading edge, we hypothesized that APPL1 regulates the amount of active Akt in adhesions. We addressed this by coimmunostaining control and APPL1-expressing cells for active Akt, using the phospho–Thr-308-Akt antibody, and paxillin. Individual paxillin-containing adhesions were visualized using total internal reflection fluorescence (TIRF) microscopy, and the levels of active Akt were quantified in these adhesions. The amount of active Akt in adhesions in APPL1-expressing cells was decreased 1.7-fold as compared with that observed in control cells (Figure 7, A and B). This result suggests that APPL1 regulates cell migration and adhesion turnover by reducing the amount of active Akt in adhesions.

APPL1 regulates the tyrosine phosphorylation of Akt by Src

Because tyrosine phosphorylation of Akt by Src was recently shown to be important in both the activation of Akt and its biological function (Chen *et al.*, 2001; Choudhury *et al.*, 2006; Bouchard *et al.*, 2007), we hypothesized that Src-mediated tyrosine phosphorylation of Akt was critical for its effects on migration. We began to test this hypothesis by assessing tyrosine phosphorylation of Akt by Src in HT1080 cells. Wild-type HT1080 cells were transfected with FLAG-Akt and subsequently treated with various concentrations of the Src family kinase inhibitor PP2. Treatment with 1 μM PP2 decreased Akt tyrosine phosphorylation by 1.8-fold compared with dimethyl sulfoxide controls, whereas 7.5 μM PP2 decreased the levels of tyrosine phosphorylation by 4.6-fold (Figure 8A). To further support a role for Src in Akt tyrosine phosphorylation, we transfected HT1080 cells with constitutively active Src (CA-Src). Expression of CA-Src resulted in a 10-fold increase in the amount of Akt tyrosine phosphorylation compared with controls (Figure 8B), suggesting a critical role for Src in mediating Akt tyrosine phosphorylation.

We next assessed the ability of APPL1 to regulate Akt tyrosine phosphorylation. When APPL1 was coexpressed with FLAG-Akt in HT1080 cells, tyrosine phosphorylation of Akt was decreased 1.9-fold compared with control cells (Figure 8C). Moreover, expression of APPL1 with CA-Src reduced Akt tyrosine phosphorylation by 2.4-fold (Figure 8D). Collectively, these data point to an important new function for APPL1 in regulating the Src-mediated tyrosine phosphorylation of Akt.

Src-mediated tyrosine phosphorylation of Akt is critical for its activation and function

Since our data indicated that APPL1 regulates the amount of active Akt in cells, we thought that it may be through a mechanism that

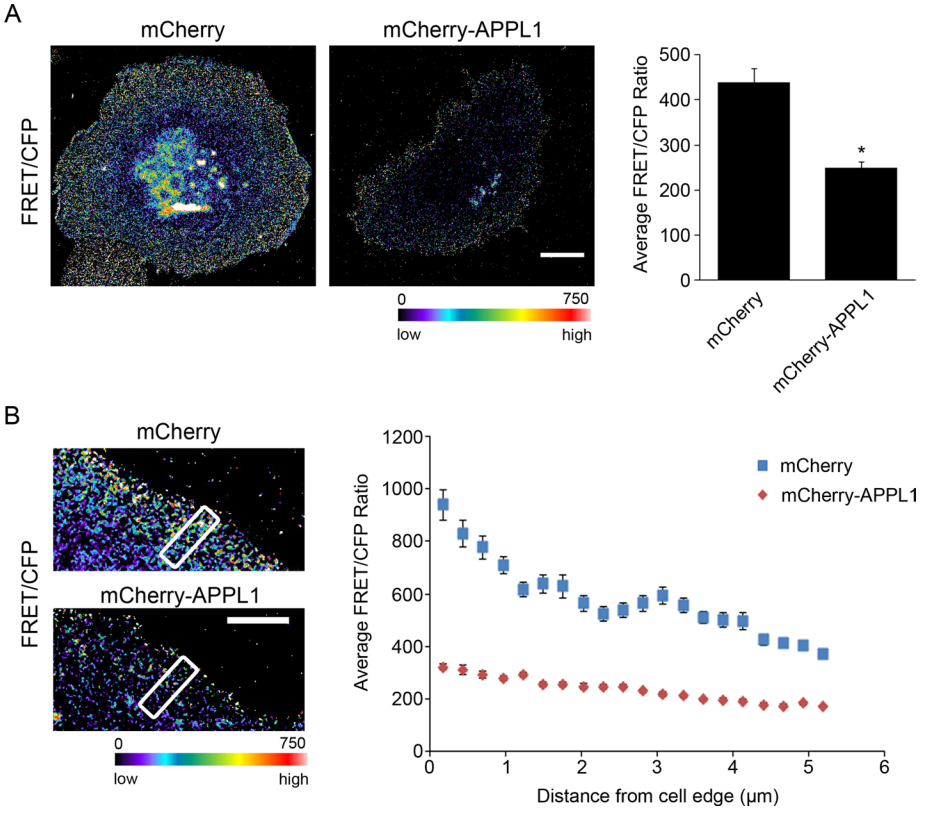

FIGURE 6: APPL1 decreases Akt activity in cells. (A) HT1080 cells were cotransfected with either mCherry or mCherry-APPL1 and the Akt activity FRET probe Akind. Ratio images of FRET/CFP are shown in pseudocolor coding (left). Scale bar, 10 μm. Quantification of the average FRET/CFP ratio for cells cotransfected with either mCherry or mCherry-APPL1 and Akind is shown (right). Error bars represent the SEM from >34 cells from at least three individual experiments (*$p < 0.0001$). (B) HT1080 cells were cotransfected with either mCherry or mCherry-APPL1 and Akind. Ratio images of FRET/CFP at the cell edge are shown in pseudocolor coding (left). Scale bar, 5 μm. A line-scan analysis was performed on the boxed region, which represents an area 5 μm long and 1.3 μm wide. Quantification of the line-scan analysis is shown (right). Error bars represent the SEM of 52–59 total line scans from 20 cells from three separate experiments.

involves Src and the tyrosine phosphorylation of Akt. In initial experiments, we assessed the ability of APPL1 and Src to regulate Akt T308 phosphorylation. Expression of APPL1 led to a 1.5-fold reduction in Akt T308 phosphorylation as compared with control cells, which confirmed our previous experiments showing that APPL1 decreases the amount of active Akt (Figure 9A). We next examined the effects of Src activity on Akt T308 phosphorylation. Expression of CA-Src resulted in a fourfold increase in Akt T308 phosphorylation (Figure 9A). However, when APPL1 was coexpressed with CA-Src in HT1080 cells, Akt T308 phosphorylation was decreased significantly compared with that observed in cells expressing CA-Src (Figure 9A). Thus, these results suggest APPL1 reduces the amount of active Akt in cells by inhibiting tyrosine phosphorylation of Akt by Src.

Because previous work showed that the major Src phosphorylation sites in Akt, which are important in regulating its activity and function, are tyrosines 315 and 326 (Chen *et al.*, 2001), we mutated these tyrosine residues to phenylalanines. In cells expressing the Akt tyrosine mutant (Akt-Y315F/Y326F), a 1.6-fold decrease in tyrosine phosphorylation was observed compared with that seen in wild-type Akt (Wt-Akt)–expressing cells (Figure 9B). In addition, the CA-Src-mediated increase in Akt tyrosine phosphorylation was reduced by 1.7-fold in cells expressing Akt-Y315F/Y326F compared with Wt-Akt–expressing cells (Figure 9C). These results suggest that residues 315 and 326 are major targets of phosphorylation by Src.

Next we assessed the importance of phosphorylation at tyrosines 315 and 326 in regulating Akt-mediated migration. Consistent with our previous data, expression of CA-Akt in HT1080 cells promoted a 1.2-fold increase in the migration speed compared with controls (Figure 9D). In contrast, mutation of tyrosines 315 and 326 in CA-Akt significantly reduced the migration of HT1080 cells. The migration speed of cells expressing CA-Akt-Y315F/Y326F was decreased 1.5-fold compared with that observed in control cells (Figure 9D). Taken together, these results indicate that tyrosine phosphorylation by Src is a critical regulator of Akt-mediated cell migration, and APPL1 inhibits migration by decreasing this tyrosine phosphorylation.

DISCUSSION

Although the signaling adaptor APPL1 has been implicated in the modulation of various cellular processes, such as proliferation and survival (Liu *et al.*, 2002; Schenck *et al.*, 2008), its role in controlling cell migration is not well understood. Here we show that APPL1 impairs the migration of HT1080 cells by regulating the assembly and disassembly of leading edge adhesions. APPL1 modulates migration and adhesion dynamics through a molecular mechanism that depends on the Src-mediated tyrosine phosphorylation of Akt. APPL1 was recently shown to affect the ability of murine embryonic fibroblasts (MEFs) to migrate in response to hepatocyte growth factor (HGF) (Tan *et al.*, 2010), which is consistent with our data indicating that it is an important modulator of this process. Intriguingly, this study found that APPL1 was dispensable for the survival of MEFs, at least under normal culture conditions (Tan *et al.*, 2010).

Our results indicate that APPL1 regulates cell migration through its multifunctional domains, which mediate its interaction with other proteins, as well as with lipids. When the PTB domain of APPL1 is deleted, it is unable to inhibit migration in HT1080 cells. This region of APPL1 was shown to be important in its binding to Akt (Mitsuuchi *et al.*, 1999), suggesting that APPL1 modulates migration through Akt. Nevertheless, we cannot rule out contributions from other APPL1-interacting proteins, since the tumor suppressor DCC, human follicle-stimulating hormone receptor, the neurotrophin receptor TrkA, and the TrkA-interacting protein GIPC1 have also been shown to bind to this region of APPL1 (Liu *et al.*, 2002; Nechamen *et al.*, 2004; Lin *et al.*, 2006). However, we provide additional results that strongly demonstrate APPL1 regulates migration by modulating Akt activity and function.

We show that Akt is a positive regulator of migration in HT1080 cells, in which CA-Akt increases migration speed, whereas DN-Akt and knockdown of endogenous Akt both decrease migration. When APPL1 is exogenously expressed with CA-Akt (threefold over endogenous), it abolishes the CA-Akt–promoted increase in migration, indicating that APPL1 inhibits Akt function. In contrast,

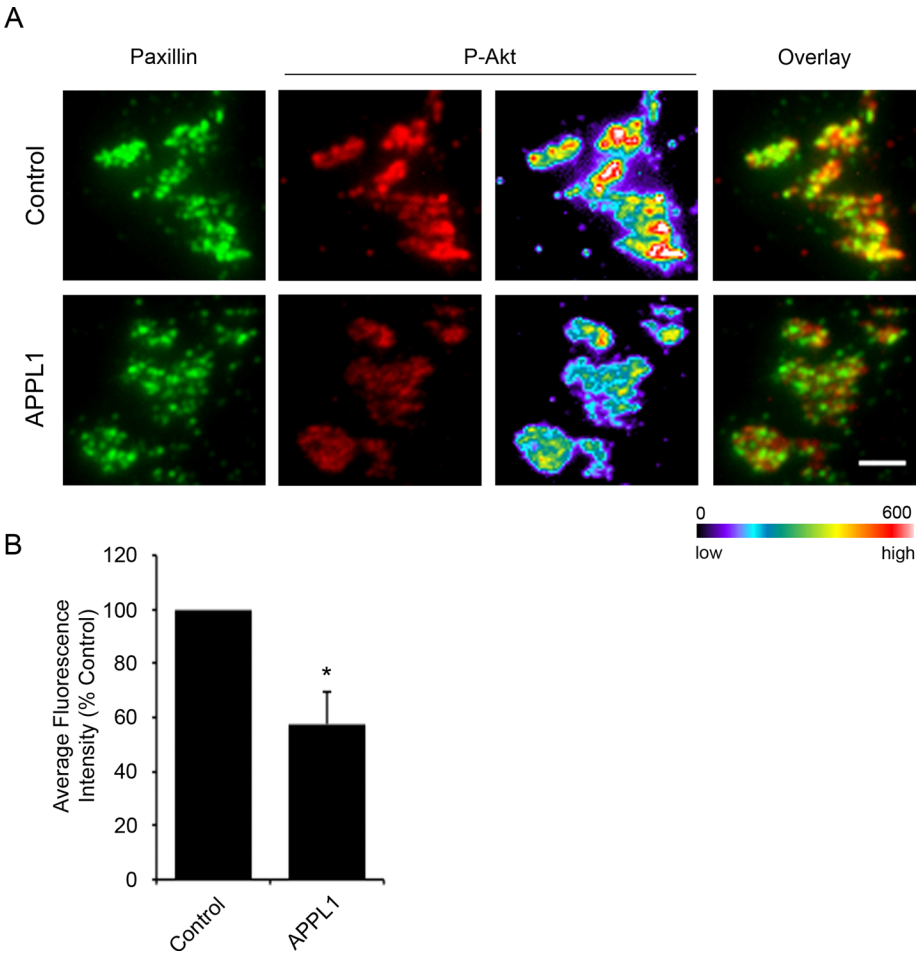

FIGURE 7: APPL1 reduces the amount of active Akt in adhesions. (A) HT1080 cells were transfected with CFP and either empty vector (Control) or FLAG-APPL1 (APPL1), fixed, and immunostained for active Akt, using a phospho-Thr-308–specific antibody (P-Akt), and paxillin. TIRF images of paxillin (left) and P-Akt (middle) are shown. P-Akt images are shown in pseudocolor coding that indicates the range of fluorescence intensities to the assigned color (P-Akt; right). Overlays of paxillin and P-Akt are shown (far right). Scale bar, 2 μm. (B) Quantification of phospho–Thr-308 Akt levels in adhesions in cells transfected with the constructs from A . Error bars represent the SEM of >4782 adhesions from 58–63 cells from three separate experiments (*p = 0.0251).

increasing the amount of CA-Akt (fivefold over endogenous) negates this effect of APPL1, demonstrating that higher expression of CA-Akt can overcome this inhibition. When APPL1 is coexpressed with either DN-Akt or in Akt knockdown cells, no further decrease in migration is observed, suggesting that APPL1 and Akt are in the same signaling pathway that regulates migration. This role of Akt in promoting cell migration is consistent with previous studies (Kim *et al.*, 2001; Irie *et al.*, 2005; Ju *et al.*, 2007; Bristow *et al.*, 2009). Interestingly, some previous studies looking at the relationship between APPL1 and Akt showed APPL1 to be a positive regulator of Akt activation (Nechamen *et al.*, 2004; Lin *et al.*, 2006; Saito *et al.*, 2007; Cheng *et al.*, 2009; Wen *et al.*, 2010), whereas our results indicate that APPL1 decreases the amount of active Akt. This discrepancy may be due, at least in part, to the isoform of Akt being observed. The major isoform of Akt in HT1080 cells is Akt1 (Supplemental Figure S4), whereas most of the previous work was focused on insulin/Akt2 signaling or on signaling in the nervous system, where Akt3 is the major isoform. Indeed, recent work has shown that APPL1 inhibits Akt1 activity (Bohdanowicz *et al.*, 2011; Tu *et al.*, 2011).

Several residues (147, 153, and 155) within the BAR domain of APPL1 are essential for its ability to regulate cell migration. The BAR domain of APPL1 is structurally unique, in that it interacts with the PH domain to form a functional unit (Li *et al.*, 2007; Zhu *et al.*, 2007). This integrated functional dimer interacts with the endosomal protein Rab5 and is responsible for APPL1's endosomal localization (Miaczynska *et al.*, 2004; Li *et al.*, 2007; Zhu *et al.*, 2007). The endosomal localization is important for APPL1 to regulate Akt substrate specificity (Schenck *et al.*, 2008), suggesting that APPL1 signaling on endosomes is critical to its function. Indeed, our results indicate that APPL1 localization to endosomal membranes is critical for its ability to regulate cell migration through Src and Akt. Akt activation, which is typically believed to occur at the plasma membrane, has also been shown to take place on signaling endosomes (Wang *et al.*, 2002). In this context, APPL1 may function as a scaffold for bringing signaling proteins to endosomal structures, which can be targeted to specific regions within the cell in a spatiotemporal manner.

Although several adaptor proteins have recently been reported to regulate processes underlying migration, namely adhesion dynamics (Nayal *et al.*, 2006; Zaidel-Bar *et al.*, 2007; Kanchanawong *et al.*, 2010), the importance of APPL1 in contributing to this process is unknown. We show that APPL1 is a negative regulator of adhesion turnover, where exogenous expression of APPL1 increases the apparent $t_{1/2}$ for adhesion assembly, as well as the $t_{1/2}$ for adhesion disassembly. Knockdown of endogenous APPL1 has the opposite effect on adhesion turnover. This phenotype depends on the PTB domain of APPL1, as expression of the APPL1-ΔPTB mutant has no effect on adhesion turnover. The dependence on the PTB domain suggests that Akt contributes to the APPL1-mediated regulation of adhesion turnover. Indeed, we previously demonstrated a potential role for Akt in regulating adhesion dynamics (Bristow *et al.*, 2009) and show here that expression of CA-Akt stimulates more rapid adhesion turnover, whereas DN-Akt induces slower turnover. Coexpression of exogenous APPL1 with CA-Akt negates the CA-Akt–promoted increase in adhesion turnover, whereas coexpression with DN-Akt has no additional effect. Moreover, expression of APPL1 causes a decrease in the amount of active Akt at the cell edge, as well as in adhesions. Thus, APPL1 may regulate the assembly and disassembly of adhesions at the leading edge by inhibiting Akt function. This would lead to impaired turnover of leading edge adhesions, which could significantly slow cell migration.

Phosphorylation at threonine 308 and serine 473 has classically been believed to activate Akt (Alessi *et al.*, 1996). However, more recent work indicates that Akt activity is also regulated by tyrosine phosphorylation, which is carried out by Src (Chen *et al.*, 2001). In our study, inhibition of Src with PP2 led to a decrease in the tyrosine

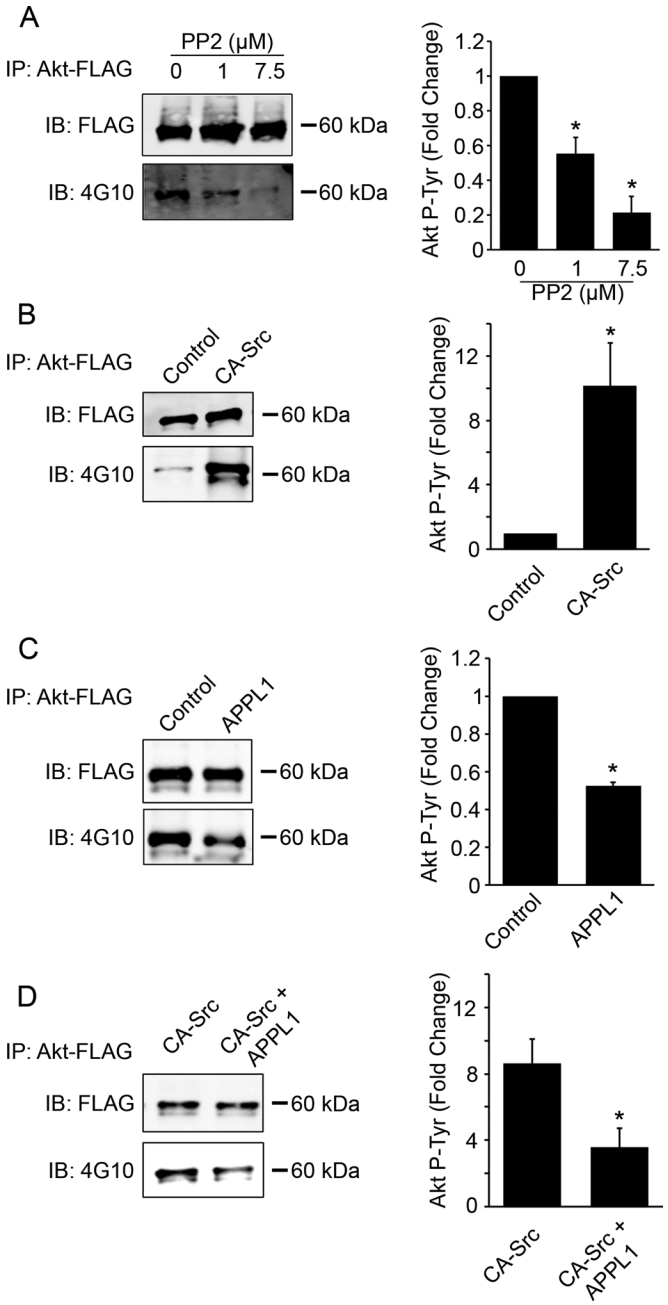

FIGURE 8: Src mediates tyrosine phosphorylation of Akt. (A) FLAG-Akt transfected HT1080 cells were incubated with the indicated concentrations of PP2 for 1.5 h. Left, FLAG-Akt protein was immunoprecipitated from cell lysates, and FLAG-Akt samples were subjected to immunoblot analysis to determine the levels of total FLAG-Akt, using FLAG M2 antibody (FLAG), and tyrosine phosphorylated Akt with 4G10 monoclonal antibody (4G10). Right, quantification of the amount of Akt tyrosine phosphorylation relative to the control (0 μM PP2). Error bars represent the SEM from three separate experiments (*$p \leq 0.0031$). (B) HT1080 cells were cotransfected with FLAG-Akt and either GFP (Control) or GFP-CA-Src (CA-Src). Left, immunoprecipitated FLAG-Akt protein samples were immunoblotted for total FLAG-Akt (FLAG) and tyrosine phosphorylated Akt (4G10). Right, quantification of the relative amount of Akt tyrosine phosphorylation compared with control. Error bars represent the SEM from three separate experiments (*$p = 0.025$). (C) FLAG-Akt was immunoprecipitated from lysates of cells expressing FLAG-Akt and either GFP (Control) or GFP-APPL1 (APPL1). Left, samples were subjected to immunoblot analysis to determine the levels of total FLAG-Akt (FLAG) and tyrosine phosphorylated Akt (4G10). Right, quantification of the relative amount of Akt tyrosine phosphorylation compared with control. Error bars represent the SEM from three separate experiments (*$p \leq 0.0001$). (D) HT1080 cells were cotransfected with FLAG-Akt and either mCherry + GFP-CA-Src (CA-Src) or mCherry-APPL1 + GFP-CA-Src (CA-Src + APPL1). Left, immunoprecipitated FLAG-Akt protein samples were subjected to immunoblot analysis to determine the levels of total FLAG-Akt (FLAG) and tyrosine phosphorylated Akt (4G10). Right, quantification of the relative amount of Akt tyrosine phosphorylation compared to that observed in control cells from B. Error bars represent the SEM from three separate experiments (*$p = 0.048$). Asterisk indicates a statistically significant difference compared with CA-Src–transfected cells.

phosphorylation of Akt, whereas promotion of Src activity, through expression of CA-Src, increased the level of tyrosine phosphorylated Akt, indicating that Src can tyrosine phosphorylate Akt. In addition, APPL1 decreased tyrosine phosphorylation of Akt and inhibited the CA-Src–promoted increase in Akt tyrosine phosphorylation. These alterations in tyrosine phosphorylation are accompanied by corresponding changes in T308 phosphorylation of Akt, which had not been previously shown. Moreover, mutation of two previously described Src phosphorylation targets (tyrosines 315 and 326; Chen *et al.*, 2001) to phenylalanines in CA-Akt reduced migration similarly to that observed with coexpression of APPL1 with CA-Akt. Thus, APPL1 can inhibit Akt function by reducing the tyrosine phosphorylation of Akt by Src, which hinders cell migration.

Our results support a working model in which the adaptor protein APPL1 inhibits cell migration and adhesion dynamics through a mechanism involving the Src-mediated tyrosine phosphorylation of Akt. Tyrosine phosphorylation of Akt by Src enhances the activity of Akt. APPL1, in turn, decreases the amount of active Akt in adhesions and at the cell edge by reducing Akt tyrosine phosphorylation. This leads to an inhibition of Akt function, particularly within regions of cells where Akt activity is high, such as the cell edge and adhesions. As a result, the ability of cells to turn over their adhesions is diminished, which leads to an impairment of cell migration.

MATERIALS AND METHODS

Reagents

An APPL1 rabbit polyclonal antibody was made using the peptides CSQSEESDLGEEGKKRESEA and CSQSEESDLGEGGKKRESEA (21st Century Biochemicals, Marlboro, MA). Primary antibodies used for this study include phosphorylated Akt (Thr-308) polyclonal antibody (Santa Cruz Biotechnology, Santa Cruz, CA), pan-Akt C67E7, Akt1 C73H10, Akt2 D6G4, and Akt3 62A8 monoclonal antibodies (Cell Signaling, Beverly, MA), paxillin monoclonal antibody (BD Bioscience PharMingen, San Diego, CA), phosphotyrosine clone 4G10 monoclonal antibody (Millipore, Billerica, MA), β-actin clone AC-15 monoclonal antibody, and FLAG M2 monoclonal antibody (Sigma-Aldrich, St. Louis, MO). Secondary antibodies used for immunocytochemistry were Alexa Fluor 488 and 555 anti-rabbit as well as Alexa Fluor 488 and 555 anti-mouse (Molecular Probes, Eugene, OR). Secondary antibodies for Western blot analysis included IRDye 800 anti-mouse and 800 anti-rabbit (Rockland Immunochemicals, Gilbertsville, PA). Fibronectin was purchased from Sigma-Aldrich. Anti-FLAG M2 agarose, mouse immunoglobulin G (IgG)–agarose, and PP2 were purchased from Sigma-Aldrich.

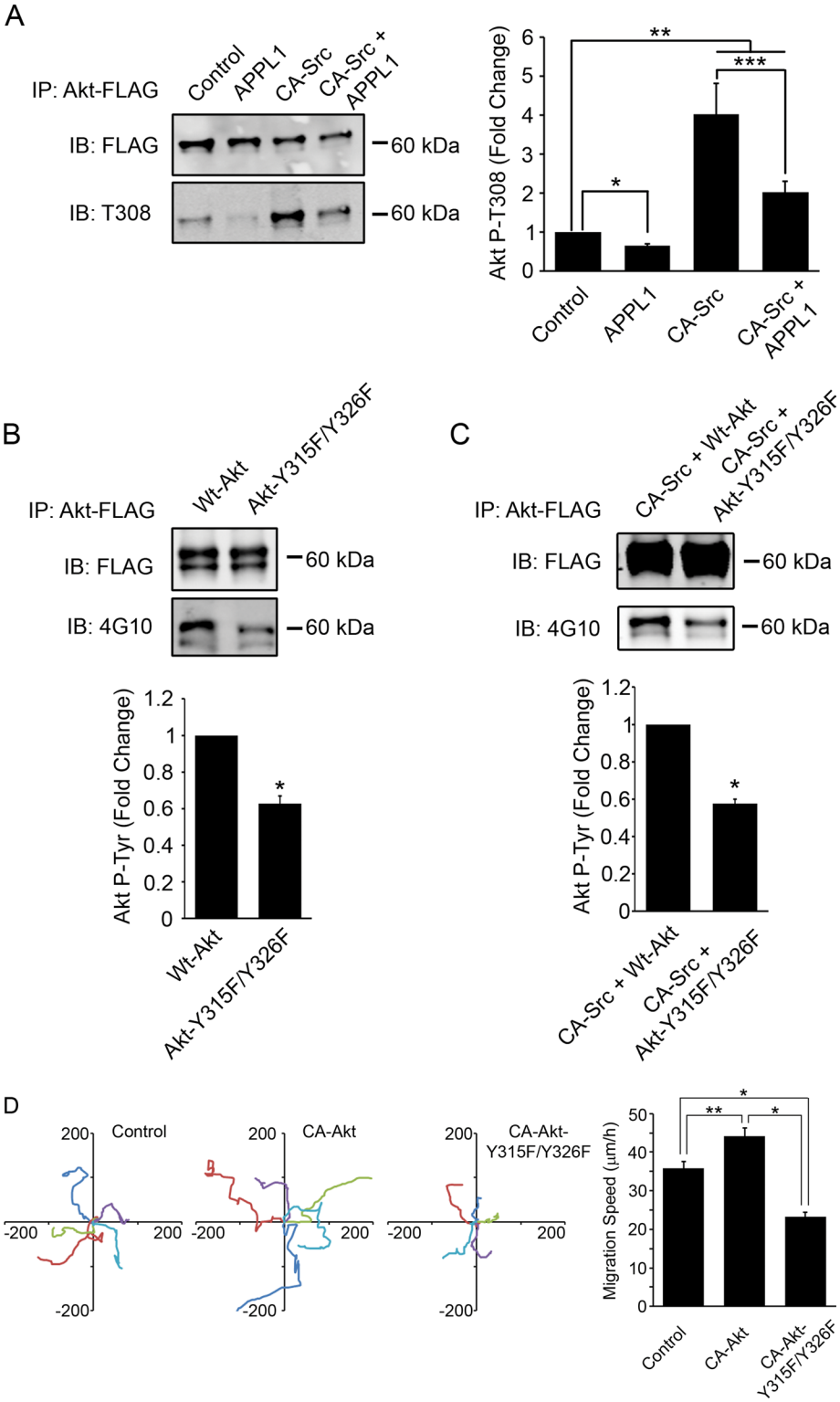

FIGURE 9: Tyrosine phosphorylation of Akt regulates its activation and function. (A) HT1080 cells were cotransfected with FLAG-Akt and mCherry + GFP (Control), mCherry-APPL1 + GFP (APPL1), mCherry + GFP-CA-Src (CA-Src), or mCherry-APPL1 + GFP-CA-Src (CA-Src + APPL1). Left, after 24 h, FLAG-Akt was immunoprecipitated from cell lysates and subjected to immunoblot analysis to determine the levels of total FLAG-Akt (FLAG) and T308 phosphorylated Akt (T308). Right, quantification of the relative amount of T308 phosphorylated Akt compared with control. Error bars represent the SEM from at least 10 separate experiments (*$p < 0.0001$, **$p \leq 0.002$, ***$p = 0.031$). (B) HT1080 cells were transfected with FLAG-Akt (Wt-Akt) or FLAG-Akt-Y315F/Y326F (Akt-Y315F/Y326F). Top, immunoprecipitated FLAG-Akt protein was subjected to immunoblot analysis to determine the levels of total FLAG-Akt (FLAG) and tyrosine phosphorylated Akt (4G10). Bottom, quantification of the relative amount of Akt tyrosine phosphorylation compared with Wt-Akt. Error bars represent the SEM from four separate experiments (*$p < 0.0001$). (C) HT1080 cells were transfected with GFP-CA-Src (CA-Src) and either FLAG-Akt (Wt-Akt) or FLAG-Akt-Y315F/Y326F (Akt-Y315F/Y326F). Top, after 24 h, FLAG-Akt protein was immunoprecipitated from cell lysates, and samples were subjected to immunoblot analysis to determine the levels of total FLAG-Akt (FLAG) and tyrosine phosphorylated Akt (4G10) . Bottom, quantification of the relative amount of Akt tyrosine phosphorylation compared with that observed in cells transfected with Wt-Akt + CA-Src. Error bars represent the SEM from three separate experiments (*$p < 0.0001$). (D) HT1080 cells were cotransfected with GFP and empty vector (Control), constitutively active Akt (CA-Akt), or CA-Akt-Y315F/Y326F and used in migration assays. Left, Rose plots with migration tracks for these cells. Right, quantification of the migration speed for cells transfected with the indicated constructs. Error bars represent the SEM for at least 56 cells from at least three separate experiments (*$p < 0.0001$, **$p = 0.0019$).

Plasmids

Full-length human APPL1 cDNA was produced via reverse transcription of HEK293 cell RNA with subsequent amplification with the SuperScript One-Step RT-PCR kit (Invitrogen, Carlsbad, CA) using the following primers: 5′-ATGCCGGGGATCGACAAGCTGCCC-3′ (forward) and 5′-TGCTTCTGATTCTCTCTTCTTTCC-3′ (reverse). Then, the APPL1 cDNA was sequenced and cloned into pEGFP-C3 vector (Clontech, Mountain View, CA). siRNA constructs were prepared as previously described (Zhang and Macara, 2008). Briefly, sense and antisense 64-mer oligonucleotides containing the 19-nucleotide targeting sequence were ligated into pSUPER vector. The siRNA oligos targeting sequences included the following: APPL1 siRNA 1, 5′-CACACCTGACCTCAAAACT-3′; APPL1 siRNA 2, 5′-AAGAGTGGATCTGTACAAT-3′; Akt siRNA 1, 5′-GGAGGGTTGGCTGCACAAA-3′; and Akt siRNA 2, 5′-CTACAACCAGGACCATGAG-3′. APPL1 siRNA 1 and both Akt target sequences have been previously described (Miaczynska *et al.*, 2004; Pore *et al.*, 2006; Degtyarev *et al.*, 2008; Bristow *et al.*, 2009). mCherry-paxillin was kindly provided by Steve Hanks (Vanderbilt University, Nashville, TN). DN-Akt1 (K179A/T308A/S473A) and CA-Akt1 (T308D/S473D) were generously provided by Brian Hemmings (Friedrich Miescher Institute, Basel, Switzerland) and Jeffrey Field (University of Pennsylvania, Philadelphia, PA). The Akind FRET probe was kindly

provided by Michiyuki Matsuda (Kyoto University, Kyoto, Japan). GFP-Src-Y527F (CA-Src) was a generous gift from Margaret Frame (University of Edinburgh, Edinburgh, United Kingdom). The cDNA for GFP-APPL1-ΔPTB (amino acids 1–466) was generated from full-length GFP-APPL1 using PCR with the following primers: 5′-TCGAATTCGGCTTATGCCGG-3′ and 5′-TCGGTACCTGGCTACTTCCAAATCCTC-3′. The PCR product was then cloned into the pEGFP-C3 vector (Clontech) at *Eco*RI and *Kpn*I. GFP-APPL1-AAA was prepared by site-directed mutagenesis of full-length GFP-APPL1 using a QuikChange II Kit (Agilent Technologies, Santa Clara, CA). For GFP-APPL1-AAA, the following primers were used to mutate amino acids R146, K152, and K154 to alanines: 5′-CGATTAATGCATATAGCCGTTTATCAGCAAAAGCAGAAAATGACAAGG-3′ and 5′-GCGATTAATGCATATAGCCGTTTATCAGCAAAAAGAG-3′. HA-FLAG-Akt1 was purchased from Addgene (Cambridge, MA). Akt-Y315F/Y326F and Akt-T308D/S473D/Y315F/Y326F were generated by site-directed mutagenesis of HA-FLAG-Akt1 using a QuikChange II Kit. For Akt-T308D/S473D/Y315F/Y326F, the following primers were used: T308D, 5′-GGTGCCACCATGAAGGACTTTTGCGGCACA-3′; Y315F, 5′-GGCACACCTGAGTTCCTGGCCCCCGAGGTG-3′; Y326F, 5′-CACTGCACGGCCGAAGTCATTGTCCTCCAG-3′; and S473D, 5′-TTCCCCCAGTTCGACTACTCGGCCAGCGGC-3′.

Cell culture, transfection, and immunoprecipitation

HT1080 cells were maintained in DMEM (Dulbecco's modified Eagle's medium; Invitrogen) with 10% fetal bovine serum (FBS) (HyClone, Logan, UT) and 1% penicillin/streptomycin (Invitrogen). Cells were transiently transfected with Lipofectamine 2000 (Invitrogen) according to the manufacturer's instructions.

For immunoprecipitation of Akt, HT1080 cells were cotransfected with 0.5 µg of FLAG-Akt cDNA and various other cDNA(s) using Lipofectamine 2000. After 24 h, cells were incubated with 1 mM sodium vanadate and 2 mM H_2O_2 (peroxovanadate) in DMEM for 15 min and then lysed with 1% NP-40 in 25 mM Tris, 100 mM NaCl, with protease inhibitors, pH 7.4. In some experiments, cells were incubated with PP2 (1–7.5 µM) for 1.5 h prior to peroxovanadate treatment. Cell lysates were precleared by incubation with nonimmune mouse-IgG agarose in 25 mM Tris, 100 mM NaCl, pH 7.4, overnight at 4°C. FLAG-Akt was immunoprecipitated with anti-FLAG M2 agarose in 25 mM Tris, 100 mM NaCl, pH 7.4, for 2 h at 4°C, followed by elution with 0.2 mg/ml FLAG peptide (Sigma-Aldrich) in 25 mM Tris, pH 7.4.

Migration assay and microscopy

Cells were plated on tissue culture dishes, which were coated with 2.5 µg/ml fibronectin for 1 h at 37°C, and permitted to adhere for 1 h at 37°C in culture media. Then cells were imaged using phase contrast microscopy on an inverted Olympus IX71 microscope (Melville, NY) with a 10× objective (numerical aperture [NA] 0.3) and a Retiga EXi CCD camera (QImaging, Surrey, Canada). Cells were kept at 37°C in CCM1 (HyClone) supplemented with 2% FBS (HyClone) at pH 7.4 during imaging. Images were acquired at 5 min intervals for at least 6 h, using MetaMorph software (Molecular Devices, Sunnyvale, CA). Cell movement was tracked from the time-lapse images using MetaMorph, and migration speed was calculated by dividing the total distance moved in microns by the time. Wind-Rose plots were generated by transposing *x*, *y* coordinates of cell tracks to a common origin.

Immunocytochemistry and image analysis

Cells were incubated on glass coverslips, which were coated with 2.5 µg/ml fibronectin, for 1 h at 37°C and subsequently fixed in either 4% paraformaldehyde with 4% glucose in phosphate-buffered saline (PBS) for 15 min at room temperature or methanol for 5 min on ice. After fixation, cells were permeabilized by incubation with 0.2% (vol/vol) Triton X-100 for 3 min and then blocked with 20% goat serum in PBS. Following blocking, appropriate primary and second antibodies, diluted in 5% goat serum with 0.2% Triton-X-100 in PBS, were added to the coverslips. After each step, coverslips were rinsed three times with PBS. Coverslips were then mounted using Aqua Poly/Mount (Polysciences, Warrington, PA). Images were acquired using MetaMorph software and an Olympus PlanApo 60× OTIRFM objective (NA 1.45). TIRF images were acquired by exciting with either a 488- or 543-nm laser line from a HeNe laser (Prairie Technologies, Middleton, WI). For GFP and Alexa Fluor 488, an Endow GFP Bandpass filter cube (excitation HQ470/40, emission HQ525/50, Q495LP dichroic mirror; Chroma, Brattleboro, VT) was used. A TRITC/Cy3 cube (excitation HQ545/30, emission HQ610/75, Q570LP dichroic mirror) was used for mCherry and Alexa Fluor 555. An ET-CFP filter cube (excitation ET436/20, emission ET480/40, T455LP dichroic mirror) was used for CFP. For TIRF imaging, a z488/543 rpc filter was used.

For quantification of phosphorylated Akt (Thr-308), the background-subtracted, integrated fluorescence intensity from individual cells was measured and normalized to the unit area using MetaMorph software. Phosphorylated Akt (Thr-308) was quantified in adhesions by thresholding paxillin fluorescence staining and creating an image mask of adhesions using the Integrated Morphometry Analysis package of MetaMorph. These masks were then applied to background-subtracted TIRF images of phosphorylated Akt, and the average level of active Akt in adhesions was quantified using the Integrated Morphometry Analysis package. For this analysis, objects with an area <0.2 µm^2 were excluded because of the difficulty in distinguishing them from background puncta.

FRET image analysis

HT1080 cells were plated on fibronectin-coated glass coverslips for 1 h at 37°C and then fixed by incubation in 4% paraformaldehyde with 4% glucose in PBS for 15 min at room temperature. For ratio-based FRET imaging, CFP, RawFRET, and Venus images were obtained by laser excitation at 405 nm for CFP and RawFRET and at 514 nm for Venus. Images were acquired with a Zeiss 710 laser scanning confocal microscope attached to an Axiobserver inverted microscope with a Plan-Apochromat 63× oil immersion objective (NA 1.40). The emission settings on the Zeiss 710 microscope were set to collect the following wavelengths: CFP, 454–568 nm; Venus, 516–621 nm; and RawFRET, 516–621 nm. For CFP and RawFRET, a 405-nm dichroic was used, and for Venus, a 458/514-nm dichroic was used. Background-subtracted FRET/CFP ratio images were generated using MetaMorph software. The equation used to calculate the FRET image for our experimental conditions was FRET = RawFRET − 0.042 × Venus − 0.184 × CFP, where CFP is the image of CFP excited by the 405-nm laser, and Venus is the image of Venus excited directly by the 514-nm laser. The CFP and Venus correction factors (0.184 and 0.042, respectively) were calculated from cells expressing CFP or Venus fluorescent protein alone and imaged in the FRET channel under the same conditions as the RawFRET images (excited by the 405-nm laser). The total FRET/CFP ratio was normalized to the unit area, and the average FRET/CFP ratio per cell was calculated. Line-scan analysis was performed using MetaMorph software with a line length of 5 µm and width of 1.3 µm, and the

average FRET/CFP ratio was calculated as a function of distance from the cell edge. FRET/CFP images shown were processed with a 3 × 3 median filter using MetaMorph software to remove noise.

Adhesion turnover assay

HT1080 cells were cotransfected with 1 μg of mCherry-paxillin cDNA and 3 μg of cDNA of the indicated constructs, plated on fibronectin-coated microscopy dishes, and imaged as previously described (Bristow *et al.*, 2009). Briefly, fluorescent time-lapse images were obtained at 15 s intervals, and the $t_{1/2}$ values for adhesion assembly and disassembly were quantified (Webb *et al.*, 2004; Bristow *et al.*, 2009).

ACKNOWLEDGMENTS

We are grateful to Jeffery Field, Margaret Frame, Steve Hanks, Brian Hemmings, and Michiyuki Matsuda for providing us with reagents. We thank Lan Hu and Vanessa Hobbs for their assistance in preparing cDNA constructs. This work was supported by National Institutes of Health Grants GM092914 and MH071674 to D.J.W. J.A.B. was supported by Predoctoral Training Grant CA078136 from the National Institutes of Health. FRET imaging was conducted at the McGill University Life Sciences Complex Imaging Facility on equipment purchased with funding from the Ministère du Développement économique, Innovation et Exportation–Québec.

REFERENCES

Alessi DR, Andjelkovic M, Caudwell B, Cron P, Morrice N, Cohen P, Hemmings BA (1996). Mechanism of activation of protein kinase B by insulin and IGF-1. EMBO J 15, 6541–6551.

Arboleda MJ, Lyons JF, Kabbinavar FF, Bray MR, Snow BE, Ayala R, Danino M, Karlan BY, Slamon DJ (2003). Overexpression of AKT2/protein kinase Bbeta leads to up-regulation of beta1 integrins, increased invasion, and metastasis of human breast and ovarian cancer cells. Cancer Res 63, 196–206.

Bohdanowicz M, Balkin DM, De Camilli P, Grinstein S (2011). Recruitment of OCRL and Inpp5B to phagosomes by Rab5 and APPL1 depletes phosphoinositides and attenuates Akt signaling. Mol Biol Cell 23, 176–187.

Bouchard V *et al.* (2007). Fak/Src signaling in human intestinal epithelial cell survival and anoikis: differentiation state-specific uncoupling with the PI3-K/Akt-1 and MEK/Erk pathways. J Cell Physiol 212, 717–728.

Bristow JM, Sellers MH, Majumdar D, Anderson B, Hu L, Webb DJ (2009). The Rho-family GEF Asef2 activates Rac to modulate adhesion and actin dynamics and thereby regulate cell migration. J Cell Sci 122, 4535–4546.

Carson M, Weber A, Zigmond SH (1986). An actin-nucleating activity in polymorphonuclear leukocytes is modulated by chemotactic peptides. J Cell Biol 103, 2707–2714.

Chen R, Kim O, Yang J, Sato K, Eisenmann KM, McCarthy J, Chen H, Qiu Y (2001). Regulation of Akt/PKB activation by tyrosine phosphorylation. J Biol Chem 276, 31858–31862.

Cheng KK, Iglesias MA, Lam KS, Wang Y, Sweeney G, Zhu W, Vanhoutte PM, Kraegen EW, Xu A (2009). APPL1 potentiates insulin-mediated inhibition of hepatic glucose production and alleviates diabetes via Akt activation in mice. Cell Metab 9, 417–427.

Chial HJ, Lenart P, Chen YQ (2010). APPL proteins FRET at the BAR: direct observation of APPL1 and APPL2 BAR domain-mediated interactions on cell membranes using FRET microscopy. PLoS One 5, e12471.

Chial HJ, Wu R, Ustach CV, McPhail LC, Mobley WC, Chen YQ (2008). Membrane targeting by APPL1 and APPL2: dynamic scaffolds that oligomerize and bind phosphoinositides. Traffic 9, 215–229.

Choi CK, Vicente-Manzanares M, Zareno J, Whitmore LA, Mogilner A, Horwitz AR (2008). Actin and alpha-actinin orchestrate the assembly and maturation of nascent adhesions in a myosin II motor-independent manner. Nat Cell Biol 10, 1039–1050.

Choudhury GG, Mahimainathan L, Das F, Venkatesan B, Ghosh-Choudhury N (2006). c-Src couples PI 3 kinase/Akt and MAPK signaling to PDGF-induced DNA synthesis in mesangial cells. Cell Signal 18, 1854–1864.

Deakin NO, Turner CE (2011). Distinct roles for paxillin and Hic-5 in regulating breast cancer cell morphology, invasion and metastasis. Mol Biol Cell 22, 327–341.

Degtyarev M *et al.* (2008). Akt inhibition promotes autophagy and sensitizes PTEN-null tumors to lysosomotropic agents. J Cell Biol 183, 101–116.

Dubash AD, Menold MM, Samson T, Boulter E, Garcia-Mata R, Doughman R, Burridge K (2009). Chapter 1. Focal adhesions: new angles on an old structure. Int Rev Cell Mol Biol 277, 1–65.

Flynn DC (2001). Adaptor proteins. Oncogene 20, 6270–6272.

Franke TF, Yang SI, Chan TO, Datta K, Kazlauskas A, Morrison DK, Kaplan DR, Tsichlis PN (1995). The protein kinase encoded by the Akt proto-oncogene is a target of the PDGF-activated phosphatidylinositol 3-kinase. Cell 81, 727–736.

Habermann B (2004). The BAR-domain family of proteins: a case of bending and binding? EMBO Rep 5, 250–255.

Irie HY, Pearline RV, Grueneberg D, Hsia M, Ravichandran P, Kothari N, Natesan S, Brugge JS (2005). Distinct roles of Akt1 and Akt2 in regulating cell migration and epithelial-mesenchymal transition. J Cell Biol 171, 1023–1034.

Ju X *et al.* (2007). Akt1 governs breast cancer progression in vivo. Proc Natl Acad Sci USA 104, 7438–7443.

Kanchanawong P, Shtengel G, Pasapera AM, Ramko EB, Davidson MW, Hess HF, Waterman CM (2010). Nanoscale architecture of integrin-based cell adhesions. Nature 468, 580–584.

Kim D, Kim S, Koh H, Yoon SO, Chung AS, Cho KS, Chung J (2001). Akt/PKB promotes cancer cell invasion via increased motility and metalloproteinase production. FASEB J 15, 1953–1962.

Laukaitis CM, Webb DJ, Donais K, Horwitz AF (2001). Differential dynamics of alpha 5 integrin, paxillin, and alpha-actinin during formation and disassembly of adhesions in migrating cells. J Cell Biol 153, 1427–1440.

Li J, Mao X, Dong LQ, Liu F, Tong L (2007). Crystal structures of the BAR-PH and PTB domains of human APPL1. Structure 15, 525–533.

Lin DC, Quevedo C, Brewer NE, Bell A, Testa JR, Grimes ML, Miller FD, Kaplan DR (2006). APPL1 associates with TrkA and GIPC1 and is required for nerve growth factor-mediated signal transduction. Mol Cell Biol 26, 8928–8941.

Liu J, Yao F, Wu R, Morgan M, Thorburn A, Finley RL Jr, Chen YQ (2002). Mediation of the DCC apoptotic signal by DIP13 alpha. J Biol Chem 277, 26281–26285.

Manning BD, Cantley LC (2007). AKT/PKB signaling: navigating downstream. Cell 129, 1261–1274.

Meenderink LM, Ryzhova LM, Donato DM, Gochberg DF, Kaverina I, Hanks SK (2010). P130Cas Src-binding and substrate domains have distinct roles in sustaining focal adhesion disassembly and promoting cell migration. PLoS One 5, e13412.

Miaczynska M, Christoforidis S, Giner A, Shevchenko A, Uttenweiler-Joseph S, Habermann B, Wilm M, Parton RG, Zerial M (2004). APPL proteins link Rab5 to nuclear signal transduction via an endosomal compartment. Cell 116, 445–456.

Mitsuuchi Y, Johnson SW, Sonoda G, Tanno S, Golemis EA, Testa JR (1999). Identification of a chromosome 3p14.3-21.1 gene, APPL, encoding an adaptor molecule that interacts with the oncoprotein-serine/threonine kinase AKT2. Oncogene 18, 4891–4898.

Miyamoto S, Teramoto H, Coso OA, Gutkind JS, Burvbelo PD, Akiyama SK, Yamada KM (1995). Integrin function: molecular hierarchies of cytoskeletal and signaling molecules. J Cell Biol 131, 791–805.

Nayal A, Webb DJ, Brown CM, Schaefer EM, Vicente-Manzanares M, Horwitz AR (2006). Paxillin phosphorylation at Ser273 localizes a GIT1-PIX-PAK complex and regulates adhesion and protrusion dynamics. J Cell Biol 173, 587–589.

Nechamen CA, Thomas RM, Cohen BD, Acevedo G, Poulikakos PI, Testa JR, Dias JA (2004). Human follicle-stimulating hormone (FSH) receptor interacts with the adaptor protein APPL1 in HEK 293 cells: potential involvement of the PI3K pathway in FSH signaling. Biol Reprod 71, 629–636.

Pawson T (2007). Dynamic control of signaling by modular adaptor proteins. Curr Opin Cell Biol 19, 112–116.

Peter BJ, Kent HM, Mills IG, Vallis Y, Butler PJ, Evans PR, McMahon HT (2004). BAR domains as sensors of membrane curvature: the amphiphysin BAR structure. Science 303, 495–499.

Ponti A, Machacek M, Gupton SL, Waterman-Storer CM, Danuser G (2004). Two distinct actin networks drive the protrusion of migrating cells. Science 305, 1782–1786.

Pore N, Jiang Z, Shu HK, Bernhard E, Kao GD, Maity A (2006). Akt1 activation can augment hypoxia-inducible factor-1alpha expression by increasing protein translation through a mammalian target of rapamycin-independent pathway. Mol Cancer Res 4, 471–479.

Saito T, Jones CC, Huang S, Czech MP, Pilch PF (2007). The interaction of Akt with APPL1 is required for insulin-stimulated Glut4 translocation. J Biol Chem 282, 32280–32287.

Schenck A, Goto-Silva L, Collinet C, Rhinn M, Giner A, Habermann B, Brand M, Zerial M (2008). The endosomal protein Appl1 mediates Akt substrate specificity and cell survival in vertebrate development. Cell 133, 486–497.

Tan Y, You H, Wu C, Altomare DA, Testa JR (2010). Appl1 is dispensable for mouse development, and loss of Appl1 has growth factor-selective effects on Akt signaling in murine embryonic fibroblasts. J Biol Chem 285, 6377–6389.

Tu Q, Zhang J, Dong LQ, Saunders E, Luo E, Tang J, Chen J (2011). Adiponectin inhibits osteoclastogenesis and bone resorption via APPL1-mediated suppression of Akt1. J Biol Chem 286, 12542–12553.

von Zastrow M, Sorkin A (2007). Signaling on the endocytic pathway. Curr Opin Cell Biol 19, 436–445.

Wang Y, Pennock S, Chen X, Wang Z (2002). Endosomal signaling of epidermal growth factor receptor stimulates signal transduction pathways leading to cell survival. Mol Cell Biol 22, 7279–7290.

Webb DJ, Donais K, Whitmore LA, Thomas SM, Turner CE, Parsons JT, Horwitz AF (2004). FAK-Src signalling through paxillin, ERK and MLCK regulates adhesion disassembly. Nat Cell Biol 6, 154–161.

Wen L, Yang Y, Wang Y, Xu A, Wu D, Chen Y (2010). Appl1 is essential for the survival of *Xenopus* pancreas, duodenum, and stomach progenitor cells. Dev Dyn 239, 2198–2207.

Yoshizaki H, Mochizuki N, Gotoh Y, Matsuda M (2007). Akt-PDK1 complex mediates epidermal growth factor-induced membrane protrusion through Ral activation. Mol Biol Cell 18, 119–128.

Yu JA, Deakin NO, Turner CE (2009). Paxillin-kinase-linker tyrosine phosphorylation regulates directional cell migration. Mol Biol Cell 20, 4706–4719.

Zaidel-Bar R, Ballestrem C, Kam Z, Geiger B (2003). Early molecular events in the assembly of matrix adhesions at the leading edge of migrating cells. J Cell Sci 116, 4605–4613.

Zaidel-Bar R, Milo R, Kam Z, Geiger B (2007). A paxillin tyrosine phosphorylation switch regulates the assembly and form of cell-matrix adhesions. J Cell Sci 120, 137–148.

Zhang H, Macara IG (2008). The PAR-6 polarity protein regulates dendritic spine morphogenesis through p190 RhoGAP and the Rho GTPase. Dev Cell 14, 216–226.

Zhou GL, Tucker DF, Bae SS, Bhatheja K, Birnbaum MJ, Field J (2006). Opposing roles for Akt1 and Akt2 in Rac/Pak signaling and cell migration. J Biol Chem 281, 36443–36453.

Zhu G *et al*. (2007). Structure of the APPL1 BAR-PH domain and characterization of its interaction with Rab5. EMBO J 26, 3484–3493.